All Sciences Proceedings
http://as-proceeding.com/

3rd International Conference on Innovative Academic Studies

September 26-28, 2023 : Konya, Turkey

ICIAS
https://www.icias.net/

The Effect of Polypropylene Fiber Addition on the Compressive Strength and Ultrasonic Pulse Velocity of Low-Temperature Cured Alkali-Activated Slag

Murat Dener

Civil Eng. Dept., Bingöl University, Turkey

(mdener@bingol.edu.tr) Email of the corresponding author

Abstract **–** Portland cement (PC) has long been a predominant binder material in the construction industry, but it is also a major contributor to carbon dioxide emissions. Alkali-activated materials (AAMs) have emerged as an environmentally friendly alternative in the construction industry. AAMs are formulated by activating aluminosilicate-based materials with alkali activators, offering potential environmental benefits by reducing carbon dioxide emissions compared to traditional PC-based binders. Due to its ability for continuous hydration at low temperatures, alkali-activated slag (AAS) stands as a promising binder material for winter construction applications. High alkali dosage (Na_2O%) dosage and alkali modulus in AAS production may result in the occurrence of shrinkage cracks. This study employed 0.3% polypropylene fiber (PP) by volume to mitigate the potential negative impact of cracks, which may arise from elevated Na_2O%, on the mechanical properties of AAS. AAS mortars were manufactured with Na_2O% of 7% and 9%. Ultrasonic pulse velocity and compressive strength tests were conducted on samples aged 7 and 28 days. The results showed that the compressive strength increased with an increase in Na_2O%. The sample with 7% Na_2O% exhibited better strength development with increasing curing time compared to its 9% counterpart. There was a decrease in compressive strength with PP substitution.

Keywords – Alkali-Activated Slag, Blast Furnace Slag, Polypropylene Fiber, Low Temperature, Alkali Dosage

I. INTRODUCTION

Executing concrete work in cold winter conditions poses distinct challenges and requires the adoption of several costly and energy-intensive measures [1]. Lower curing temperatures can have adverse effects on the mechanical and durability properties of ordinary Portland cement (PC)-based composites [2]. The optimal curing temperature range for PC composites is typically 10 °C to 20 °C [3]. A minimum temperature of 5 °C is essential to sustain normal PC hydration. Below this threshold, PC hydration is delayed, resulting in a significantly slower rate of concrete strength development [4,5]. Consequently, various measures are taken in low-temperature conditions to maintain concrete within optimal curing parameters. These measures encompass heating systems and electric insulation blankets [6]. Nonetheless, these preventive systems contribute to increased energy consumption, CO_2 emissions, and operational costs [1,7]. The production of PC leads to the emission of substantial greenhouse gases, contributing to global warming, and involves significant consumption of raw materials [8]. The production of cement contributes to approximately two billion tons of greenhouse gas emissions annually, accounting for around 6% of the world's anthropogenic greenhouse gas emissions [8,9]. Alkali-activated materials (AAMs) are considered promising alternatives to PC binders due to their positive environmental impact and good technical properties [10,11]. AAMs are created by the

interaction between an amorphous solid aluminosilicate precursor and an alkali activator. Commonly employed aluminosilicate precursors encompass metakaolin, silica fume, fly ash, and blast furnace slag [12–14].

Alkali-activated slag (AAS) distinguishes itself by its capability to attain the desired strength levels without necessitating heat treatment or the incorporation of special additives [15,16]. AAS concrete can achieve compressive strengths of up to 150 MPa when cured under room temperature conditions [17]. Furthermore, the alkali activator solution contains a sufficient concentration of free ions, which notably reduces its freezing point. In theory, this makes it feasible to produce AAS pastes at lower temperatures [18]. Various studies have demonstrated the feasibility of using AAS at low temperatures [1,5,19,20].

In order to ensure satisfactory mechanical performance of AAS cured at low temperatures, it is necessary to maintain a higher alkali dosage (Na_2O%), which, in turn, leads to pronounced shrinkage [20,21]. AAS was observed to exhibit shrinkage levels up to six times greater than those of PC, as reported [21]. In comparison to PC, the C-S-H (calcium silicate hydrate) formed in AAS is denser and possesses a lower H/Si ratio [22]. Consequently, this leads to a reduced volume of products and the evaporation of excess water, resulting in significant drying shrinkage. Such shrinkage adversely impacts the material's durability and strength [23]. Incorporating fibers can be a viable approach to mitigate the development of cracks induced by shrinkage [24,25]. Xu et al. [25] reported that the addition of polypropylene fiber (PP) can effectively manage the drying shrinkage of AAS mortar. In comparison to the control sample, the incorporation of 0.2% PP led to a notable reduction of 37.1% in drying shrinkage. Akturk et al. [26] illustrated that the inclusion of PP enhanced the flexural strength of AAS mortars. Zhou et al. [24] observed a gradual enhancement in the flexural strength of fiber-reinforced AAS concrete as the dosage of basalt fiber increased.

In the context of this study, a total of four mixtures were generated. Among these, two mixtures incorporated PP, while the remaining two were formulated without fibers. This design was employed to assess the impact of fiber inclusion. The results showed that the addition of PP to AAS cured at low temperatures did not improve compressive strength but adversely affected it.

II. EXPERIMENTAL METHODS

A. Materials

Ground granulated blast furnace slag (GBFS) was employed as the precursor material. GBFS possesses a specific gravity of 2.8. The chemical composition of GBFS is outlined in Table 1. The aggregate has a specific gravity of 2.65 and a water absorption of 1.92%. The maximum grain diameter of the aggregate is 4 mm. An activator blend consisting of Na_2SiO_3 and NaOH was utilized. The Na_2SiO_3 solution is composed of 28% SiO_2, 13.5% Na_2O, and 58.4% water by weight. The NaOH pellets employed have a purity of 99%.

Table 1. The chemical composition of the GBFS.

Constituent	GBFS (wt. %)
SiO_2	40.52
Al_2O_3	13.74
MgO	7.72
CaO	33.86
Fe_2O_3	1.74
SO_3	0.17
Na_2O	0.66
K_2O	0.81

B. Mix proportions and test method

To investigate the influence of PP inclusion on the compressive strength of AAS cured at low temperature, a total of four mixtures were prepared. The mixing ratios are provided in Table 2. The ratio of sand to binder and water to binder was 2.75 and 0.45, respectively. The alkali modulus set to 1.5. Based on the outcomes of the preliminary study, alkali dosages of 7% and 9% were established.

Table 2. Mix proportions (1 m3).

Mix code	PP (vol. %)	Aggregate (kg)	GBFS (kg)
N7-0	-	1148.3	526.7
N0.7-0.3	0.3%	1148.3	526.7
N9-0	-	1438.3	523.0
N9-0.3	0.3%	1438.3	523.0
Mix code	Na_2SiO_3 (kg)	NaOH (kg)	Water (kg)
N7-0	196.9	13.3	122
N0.7-0.3	196.9	13.3	122
N9-0	251.4	16.9	88.5
N9-0.3	251.4	16.9	88.5

The mixing process was initiated by blending the solid materials for approximately thirty seconds. Subsequently, the activator mixture was added, and thorough mixing was continued until a homogeneous blend was achieved. The prepared mortar was subsequently placed into 50 mm cube molds and stored in a freezer at 2 °C until the testing days. Ultrasonic pulse velocity (UPV) testing (See Fig. 1a) was conducted following the procedures outlined in ASTM C597 [27]. The compression test (See Fig. 1b) was carried out using a universal testing machine with a consistent loading rate of 1.3 MPa/s, in accordance with the specifications of ASTM C109 [28]. Fig. 1c shows the samples prepared for tests performed after 7 days.

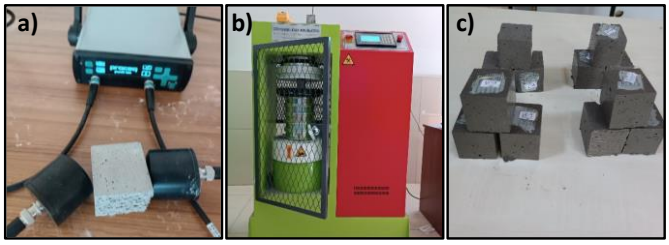

Fig. 1. a) UPV test b) compression test c) prepared samples.

III. Results and Discussion

A. *Compressive strength*

The compressive strengths of the samples at both 7 and 28 days are illustrated in Fig. 2 and Fig. 3, respectively. The results indicate that compressive strength increases with an increase in Na_2O% at a given alkali modulus. This can be attributed to a higher degree of alkali activation of GBFS at a higher Na_2O%. In other words, increasing the amount of alkali activator enhances the reactivity of the GBFS, resulting in better strength development [21,29,30]. The increase in Na_2O% resulted in a significant enhancement in early age compressive strength. The 7-day compressive strength of the sample with a 9% Na_2O% was 63.5% higher than the sample with a 7% Na_2O%. This increase can be attributed to the accelerated dissolution rate achieved by increasing Na_2O%, leading to the early formation of gel products that promote early strength development [31]. However, it's worth noting that the compressive strength of the sample with a 7% alkali dosage exhibited a remarkable improvement of 136.3% at the end of 28 days. In contrast, for the mixture with a 9% alkali dosage, this rate was 60.6%. These findings indicate that while higher Na_2O% contribute to early strength gains, there is a diminishing effect on strength enhancement over a longer curing period. The observed phenomenon can be attributed to shrinkage induced by redundant alkali activator [32].

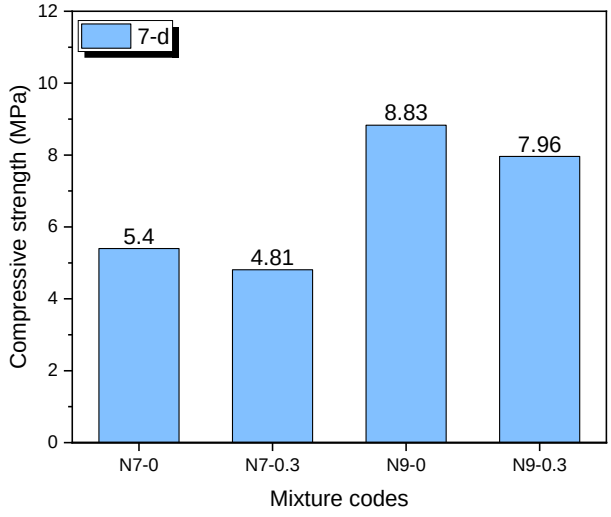

Fig. 2. Compressive strength results at the end of 7 days.

Regarding the impact of fiber utilization on the compressive strength of AAS samples cured at low temperatures, it was noted that the incorporation of PP at two different alkali dosages resulted in a reduction in compressive strength. The 7-day compressive strength of samples produced at both 7% and 9% alkali dosage decreased by approximately 10%. The addition of PP decreased the 28-day compressive strength of the sample with

7% Na_2O% from 17.76 MPa to 12.20 MPa, while it decreased the compressive strength of the sample with 9% Na_2O% from 14.18 MPa to 12.90 MPa. For AAS samples cured at low temperatures to achieve good mechanical performance, it is necessary to have a higher alkali modulus and Na_2O% compared to AAS cured at room temperatures [2]. The presence of shrinkage-induced cracks in AAS can be a concern for the mechanical performance of the material [33]. It was expected that the use of fibers, such as PP, could help mitigate these cracks and improve the compressive strength of AAS [24]. However, in the study, it was observed that the inclusion of PP fibers had a negative effect on the compressive strength of AAS cured at low temperatures. When producing AAS at low temperatures, especially by substituting a portion of the slag with materials like PC or lime, the reaction kinetics can be accelerated [2]. This can lead to the formation of more calcium silicate hydrate (C-S-H)-like gels and potentially result in increased cracking due to the rapid hydration process [19]. In such situations, the use of fibers, PP, can indeed be beneficial. The fibers can help mitigate the damage caused by advanced crack formation by providing reinforcement and bridging across cracks. This reinforcement action can enhance the compressive strength of the material and improve its overall performance, even in cases where cracking is more pronounced [24].

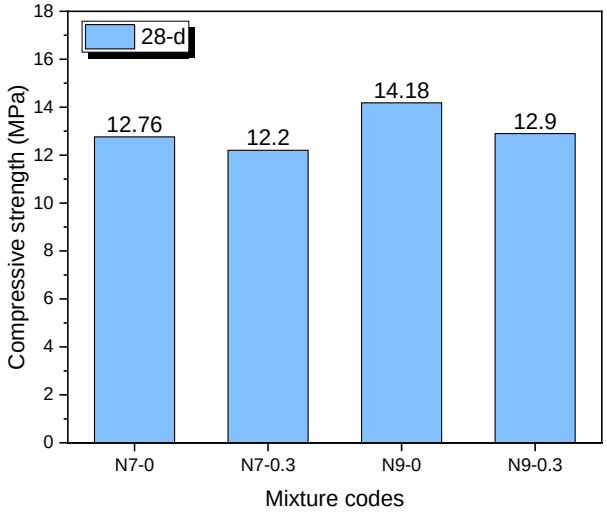

Fig. 3. Compressive strength results at the end of 28 days.

B. *Ultrasonic pulse velocity*

The UPV results of the mixtures at both 7 and 28 days are illustrated in Fig. 4 and Fig. 5, respectively. The point where the UPV results align with the compressive strength results is the decrease in UPV values associated with the addition of PP. The 7-day UPV measurement for the sample with a 7% Na_2O% showed a decline from 2717 m/s to 2577 m/s. Similarly, the UPV value of the sample with a 9% Na_2O% exhibited a reduction from 2898 m/s to 2793 m/s. The decrease in the UPV value with the addition of PP was also observed in the 28-day samples. The introduction of fibers into the material can alter its acoustic properties by affecting the path of the ultrasonic waves. The presence of fibers may scatter or attenuate the ultrasonic pulses to a certain degree, leading to lower UPV values [34,35].

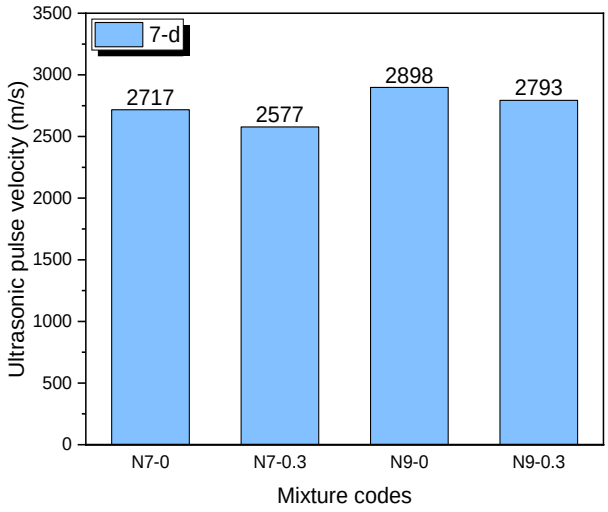

Fig. 4. UPV results at the end of 7 days.

The increase in the 7-day UPV value from 2717 m/s to 2898 m/s with an increase in Na_2O% from 7% to 9% indicates that higher alkali dosages have a positive effect on the ultrasonic properties of the AAS during early stages of curing. Higher Na_2O% can promote faster dissolution and activation of the slag particles, leading to increased early-stage hydration. This enhanced hydration can result in the formation of a more compact and less porous microstructure, which may contribute to higher UPV values [30,31]. The point where the UPV results diverged from the compressive strength results was that the UPV value decreased with the increase of the curing time. With the increase of curing time, the formation of cracks due to shrinkage caused the UPV value to decrease. Higher Na_2O% concentration may cause shrinkage and even micro cracks, compressive strength is not as sensitive to cracks as UPV [36].

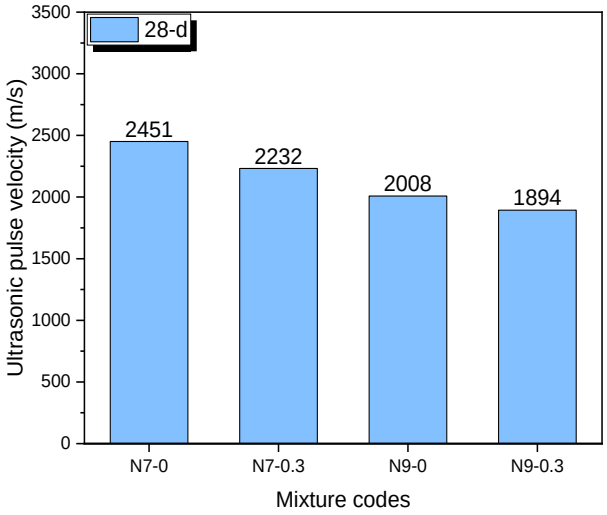

Fig. 5. UPV results at the end of 28 days.

IV. CONCLUSION

In this study, which investigated the effect of fiber utilization on the compressive strength and UPV values of AAS cured at low temperatures, the following conclusions were drawn.

- Increasing the Na_2O% from 7% to 9% led to improvements in both the 7-day and 28-day compressive strengths.
- With increasing curing time, the sample with 7% alkali dosage exhibited greater compressive strength development.
- The increase in Na_2O% resulted in an increase in the 7-day UPV value, while it led to a decrease in the UPV value measured at the end of 28 days.
- The incorporation of 0.3% fiber reduced both the compressive strength and UPV value of samples with both 7% and 9% alkali dosage.

In present study, it was observed that the use of fiber had an adverse effect on the compressive strength of AAS cured at room temperature. For future studies, it might be worthwhile to investigate the impact of using basalt fiber with higher tensile strength instead of PP on the compressive strength of AAS cured at low temperatures.

REFERENCES

[1] A. Alzaza, K. Ohenoja, M. Illikainen, Enhancing the mechanical and durability properties of subzero-cured one-part alkali-activated blast furnace slag mortar by using submicron metallurgical residue as an additive, Cem. Concr. Compos. 122 (2021) 104128. https://doi.org/10.1016/j.cemconcomp.2021.104128.

[2] G. Zhang, H. Yang, C. Ju, Y. Yang, Novel selection of environment-friendly cementitious materials for winter construction: Alkali-activated slag/Portland cement, J. Clean. Prod. 258 (2020). https://doi.org/10.1016/j.jclepro.2020.120592.

[3] C.J. Korhonen, Antifreeze admixtures for cold regions concreting: a literature review, (1990).

[4] K. Yu, M. Jia, Y. Yang, Y. Liu, A clean strategy of concrete curing in cold climate: Solar thermal energy storage based on phase change material, Appl. Energy. (2023). https://doi.org/10.1016/j.apenergy.2022.120375.

[5] H. Zhang, J. Ai, Q. Ren, X. Zhu, B. He, Z. Jiang, Understanding the strength evolution of alkali-activated slag pastes cured at subzero temperature, Cem. Concr. Compos. 138 (2023) 104993. https://doi.org/10.1016/j.cemconcomp.2023.104993.

[6] R. Polat, The effect of antifreeze additives on fresh concrete subjected to freezing and thawing cycles, Cold Reg. Sci. Technol. (2016). https://doi.org/10.1016/j.coldregions.2016.04.008.

[7] F. Karagol, R. Demirboga, W.H. Khushefati, Behavior of fresh and hardened concretes with antifreeze admixtures in deep-freeze low temperatures and exterior winter conditions, Constr. Build. Mater. (2015). https://doi.org/10.1016/j.conbuildmat.2014.12.011.

[8] A.L. Almutairi, B.A. Tayeh, A. Adesina, H.F. Isleem, A.M. Zeyad, Potential applications of geopolymer concrete in construction: A review, Case Stud. Constr. Mater. (2021). https://doi.org/10.1016/j.cscm.2021.e00733.

[9] Y.H.M. Amran, R. Alyousef, H. Alabduljabbar, M. El-Zeadani, Clean production and properties of geopolymer concrete; A review, J. Clean. Prod. (2020). https://doi.org/10.1016/j.jclepro.2019.119679.

[10] B. Zhang, H. Zhu, Y. Cheng, G.F. Huseien, K.W. Shah, Shrinkage mechanisms and shrinkage-mitigating strategies of alkali-activated slag composites: A critical review, Constr. Build. Mater. (2022). https://doi.org/10.1016/j.conbuildmat.2021.125993.

[11] M. Dener, Mechanical and durability properties of alkali-activated slag/waste basalt powder mixtures, Proc. Inst. Mech. Eng. Part L J. Mater. Des. Appl. (2023) 14644207231193616.

[12] J.L. Provis, S.A. Bernal, Geopolymers and Related Alkali-Activated Materials, Annu. Rev. Mater. Res. 44 (2014) 299–327. https://doi.org/10.1146/annurev-matsci-070813-113515.

[13] S. Çelikten, M. Sarıdemir, İ. Özgür Deneme, Mechanical and microstructural properties of alkali-activated slag and slag + fly ash mortars exposed to high temperature, Constr. Build. Mater. 217 (2019) 50–61. https://doi.org/10.1016/j.conbuildmat.2019.05.055.

[14] M. Dener, Effect of Ferrochrome Slag Substitution on High Temperature Resistance and Setting Time of Alkali-Activated Slag Mortars, Iran. J. Sci. Technol.

Trans. Civ. Eng. (2023). https://doi.org/10.1007/s40996-023-01087-w.
[15] H. Zhang, X. Shi, Q. Wang, Effect of curing condition on compressive strength of fly ash geopolymer concrete, ACI Mater. J. (2018). https://doi.org/10.14359/51701124.
[16] M. Amran, G. Murali, N.H.A. Khalid, R. Fediuk, T. Ozbakkaloglu, Y.H. Lee, S. Haruna, Y.Y. Lee, Slag uses in making an ecofriendly and sustainable concrete: A review, Constr. Build. Mater. (2021). https://doi.org/10.1016/j.conbuildmat.2020.121942.
[17] T. Bakharev, J.G. Sanjayan, Y.B. Cheng, Alkali activation of Australian slag cements, Cem. Concr. Res. 29 (1999) 113–120. https://doi.org/10.1016/S0008-8846(98)00170-7.
[18] N. Li, C. Shi, Z. Zhang, Understanding the roles of activators towards setting and hardening control of alkali-activated slag cement, Compos. Part B. 171 (2019) 34–45. https://doi.org/10.1016/j.compositesb.2019.04.024.
[19] C. Ju, Y. Liu, M. Jia, K. Yu, Z. Yu, Y. Yang, Effect of calcium oxide on mechanical properties and microstructure of alkali-activated slag composites at sub-zero temperature, J. Build. Eng. 32 (2020) 101561. https://doi.org/10.1016/j.jobe.2020.101561.
[20] G. Zhang, H. Yang, C. Ju, Y. Yang, Novel selection of environment-friendly cementitious materials for winter construction: Alkali-activated slag/Portland cement, J. Clean. Prod. (2020). https://doi.org/10.1016/j.jclepro.2020.120592.
[21] C. Duran Atiş, C. Bilim, Ö. Çelik, O. Karahan, Influence of activator on the strength and drying shrinkage of alkali-activated slag mortar, Constr. Build. Mater. 23 (2009) 548–555. https://doi.org/10.1016/j.conbuildmat.2007.10.011.
[22] J.J. Thomas, A.J. Allen, H.M. Jennings, Density and water content of nanoscale solid C-S-H formed in alkali-activated slag (AAS) paste and implications for chemical shrinkage, Cem. Concr. Res. (2012). https://doi.org/10.1016/j.cemconres.2011.11.003.
[23] M. Kheradmand, Z. Abdollahnejad, F. Pacheco-Torgal, Shrinkage Performance of Fly Ash Alkali-activated Cement Based Binder Mortars, KSCE J. Civ. Eng. (2018). https://doi.org/10.1007/s12205-017-1714-3.
[24] X. Zhou, Y. Zeng, P. Chen, Z. Jiao, W. Zheng, Mechanical properties of basalt and polypropylene fibre-reinforced alkali-activated slag concrete, Constr. Build. Mater. (2021). https://doi.org/10.1016/j.conbuildmat.2020.121284.
[25] Y. Xu, G. Xing, J. Zhao, Y. Zhang, The effect of polypropylene fiber with different length and dosage on the performance of alkali-activated slag mortar, Constr. Build. Mater. (2021). https://doi.org/10.1016/j.conbuildmat.2021.124978.
[26] B. Akturk, A.H. Akca, A.B. Kizilkanat, Fracture response of fiber-reinforced sodium carbonate activated slag mortars, Constr. Build. Mater. (2020). https://doi.org/10.1016/j.conbuildmat.2020.118128.
[27] ASTM C597, Standard Test Method for Pulse Velocity Through Concrete, Am. Soc. Test. Mater. West Conshohocken, PA, USA. (2016) 1–4. https://doi.org/10.1520/C0597-09.
[28] A. ASTM C109/C109M, Compressive Strength of Hydraulic Cement Mortars (Using 2-in . or [50-mm] Cube Specimens) 1, Am. Soc. Test. Mater. (2007).
[29] F. Puertas, S. Martínez-Ramírez, S. Alonso, T. Vázquez, Alkali-activated fly ash/slag cements. Strength behaviour and hydration products, Cem. Concr. Res. 30 (2000) 1625–1632. https://doi.org/10.1016/S0008-8846(00)00298-2.
[30] Z. Shi, C. Shi, S. Wan, N. Li, Z. Zhang, Effect of alkali dosage and silicate modulus on carbonation of alkali-activated slag mortars, Cem. Concr. Res. (2018). https://doi.org/10.1016/j.cemconres.2018.07.005.
[31] A.E. Abubakr, A.M. Soliman, S.H. Diab, Effect of activator nature on the impact behaviour of Alkali-Activated slag mortar, Constr. Build. Mater. 257 (2020) 119531. https://doi.org/10.1016/j.conbuildmat.2020.119531.
[32] F. Collins, J.G. Sanjayan, Effect of pore size distribution on drying shrinking of alkali-activated slag concrete, Cem. Concr. Res. 30 (2000) 1401–1406.
[33] D.E. Angulo-Ramírez, R. Mejía de Gutiérrez, F. Puertas, Alkali-activated Portland blast-furnace slag cement: Mechanical properties and hydration, Constr. Build. Mater. 140 (2017) 119–128. https://doi.org/10.1016/j.conbuildmat.2017.02.092.
[34] K. Ono, A Comprehensive Report on Ultrasonic Attenuation of Engineering Materials , Including Metals , Ceramics , Appl. Sci. (2020).
[35] N.I. Zulkifli, A. Alisibramulisi, N. Saari, R. Hassan, E. Shaffie, N. Mohamad Bhkari, M.N. Muhd Sidek, Experimental Investigation of Ultrasonic Pulse Velocity (UPV) Test Specimen in Assessing the Strength of Steel Fiber Reinforced Concrete Structure, J. Adv. Ind. Technol. Appl. (2021). https://doi.org/10.30880/jaita.2021.02.02.004.
[36] S. Fang, E.S.S. Lam, B. Li, B. Wu, Effect of alkali contents, moduli and curing time on engineering properties of alkali activated slag, Constr. Build. Mater. 249 (2020). https://doi.org/10.1016/j.conbuildmat.2020.118799.